

Functional genomic profiling of O-GlcNAc reveals its context-specific interplay with RNA polymerase II

Sofia Rucli^{1,2,3}, Nicolas Descostes^{1,3}, Yulia Ermakova¹, Urvashi Chitnavis¹, Jeanne Couturier¹, Ana Boskovic¹, Matthieu Boulard^{1,*}

¹ Epigenetics & Neurobiology Unit, EMBL Rome, European Molecular Biology Laboratory, Italy

² Collaboration for a joint PhD degree between EMBL and Heidelberg University, Germany

³ These authors contributed equally: Sofia Rucli, Nicolas Descostes

Correspondence: matthieu.boulard@embl.it

Additional file 1:

Figures S1 to S3.

Figure S1. O-GlcNAc profiling in ESCs (pages 2-3)

Figure S2. Nuclear O-GlcNAc perturbation during ESCs' differentiation to NPCs (pages 4-5)

Figure S3. O-GlcNAc profiling after RNA Pol II degradation in DLD-1 cells (pages 6-7)

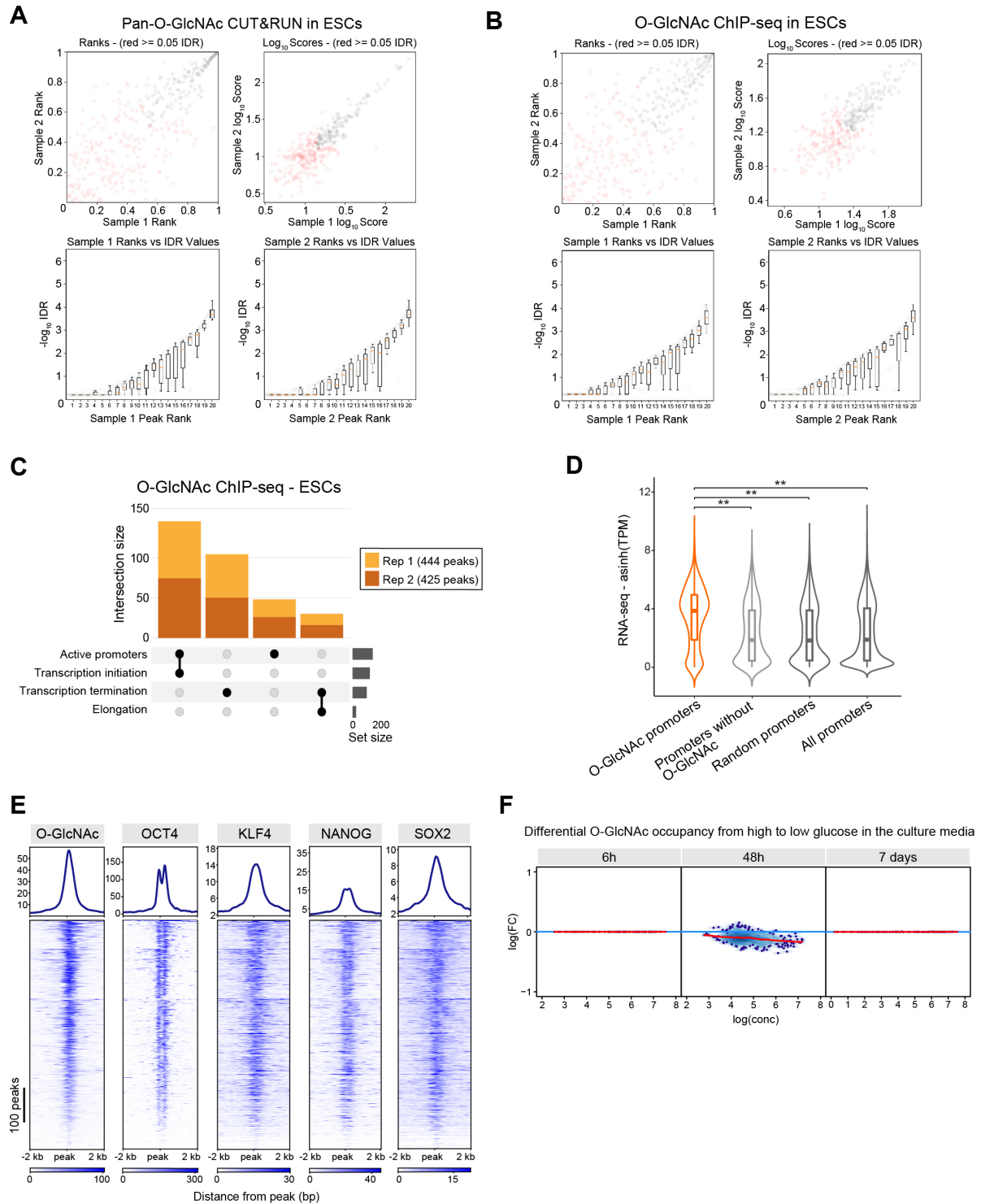


Fig. S1 O-GlcNAc profiling in ESCs (continued on page 3)

A Irreproducible Discovery Rate (IDR) of the two CUT&RUN replicates in mouse ESCs (527/523 peaks) with significant IDR < 0.05 in black. **B** Irreproducible Discovery Rate (IDR) of the two ChIP-Seq replicates in mouse ES cells (444/425 peaks) with significant IDR < 0.05 in black. **C** Upset plot of the location of O-GlcNAc ChIP-seq peaks in mouse ESC (444 and 425 peaks for replicates 1 and 2) in functional genomic compartments: Active promoters (95/101 peaks), Transcription Initiation (83/85 peaks), Transcription Termination (70/68 peaks) and

Transcription Elongation (16/19 peaks). O-GlcNAc preferentially occupies active promoters at the transcription initiation sites. **D** Violin plot showing the expression levels of genes using a publicly available RNA-seq (SRA: SRR11294181) with promoters highly occupied by O-GlcNAc (ChIP-seq) modified proteins (n=236), promoters without detectable O-GlcNAc signal (n=236), randomly selected promoters (n=236), and all promoters (n=21,085). The boundaries of the overlaid box plot show the data above the 1st and within the 3rd quartiles, whiskers indicate minimum and maximum values, the horizontal bar in the box plot shows the median. Statistical comparison was performed using a Mann-Whitney-Wilcoxon two-sided test. *: $p < 0.05$; **: $p < 0.01$. **E** Heatmap of CUT&RUN O-GlcNAc signal and ChIP-seq signal from ChIP-Atlas selected pluripotency factors previously shown to be O-GlcNAcylated, OCT4, KLF4 and SOX2, and NANOG that is not O-GlcNAc modified, +/- 1 kb around the center of O-GlcNAc peaks. The list of peaks was obtained by computing the union of the peak replicate (702 peaks). **F** Differential occupancy analysis of CUT&RUN O-GlcNAc peaks between cells grown in high glucose conditions and cells grown in low glucose for 6 h, 48 h and 7 days.

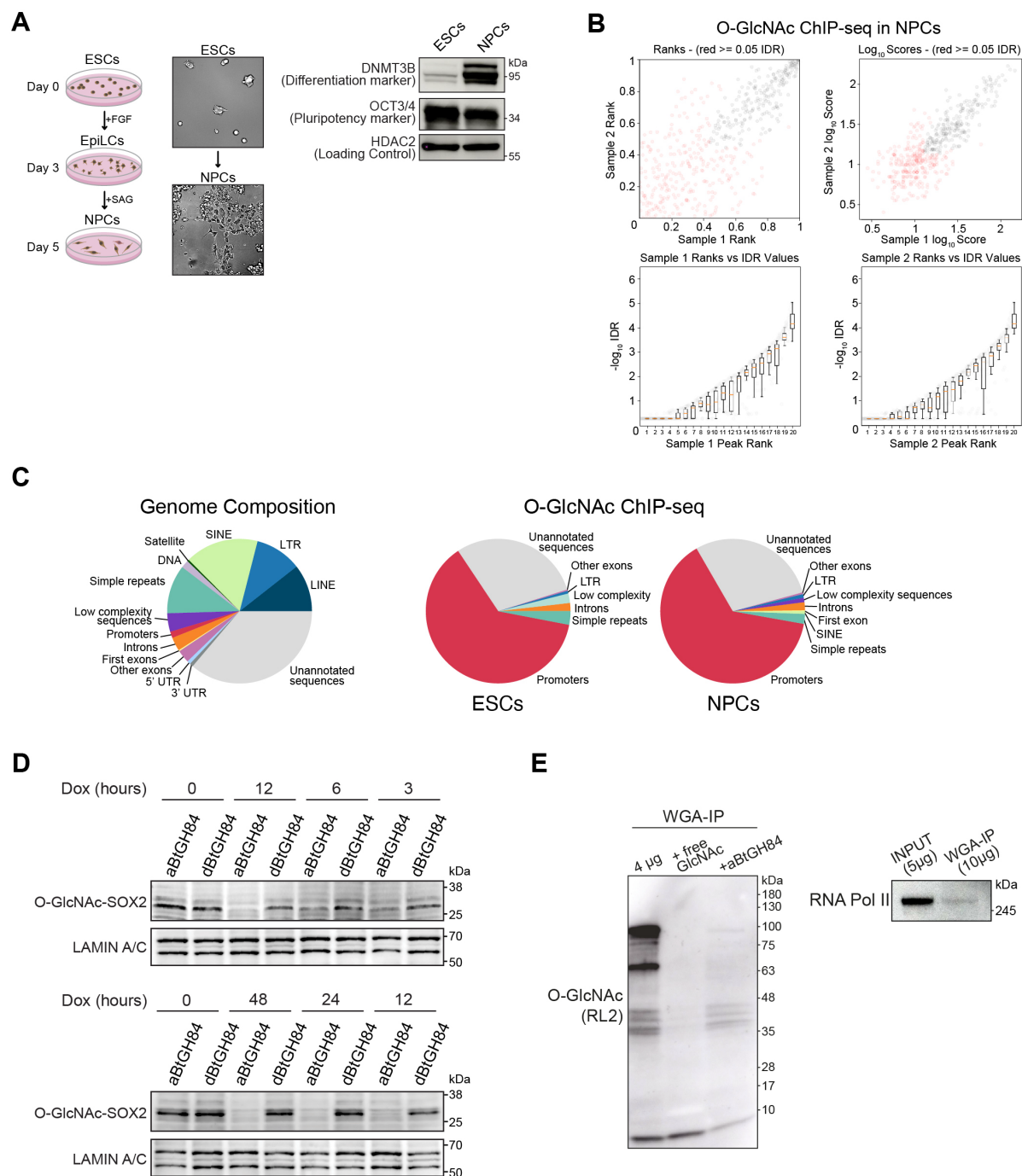


Fig. S2 Nuclear O-GlcNAc perturbation during ESCs' differentiation to NPCs (continued on page 5)

A Left: schematic representation of ESCs to NPCs differentiation protocol. Middle: representative brightfield images of ESCs before differentiation (top) and after differentiation in NPCs (bottom) cells at ESC and NPC stages. Right: Western Blot analysis of ESCs to NPCs differentiation using DNMT3B and OCT3/4 markers. **B** Irreproducible Discovery Rate (IDR) of the two ChIP-Seq replicates in mouse NPCs (640/794 peaks) with significant IDR < 0.05 in black. **C** Pie-chart showing the O-GlcNAc ChIP-seq signal distribution at different genomic loci (right) in comparison with the representative proportions of each locus in the mouse genome

(left). O-GlcNAc ChIP-seq was performed in duplicates using O-GlcNAc HGAC85 antibody in ESCs (444/425 peaks) and NPCs (640/794 peaks) and the intersection of each replicate peak was used (329 and 498 peaks). **D** Western blot detection of O-GlcNAc-modified SOX2 for the indicated time intervals following *BtGH84-NLS* induction. **E** Left: WGA-IP of nuclear O-GlcNAcylated proteins confirmed by O-GlcNAc WB analysis, in presence of large excess of free-GlcNAc and in presence of purified BtGH84 enzyme as negative controls. Right: RNA Pol II western blot detection before and after WGA-IP.

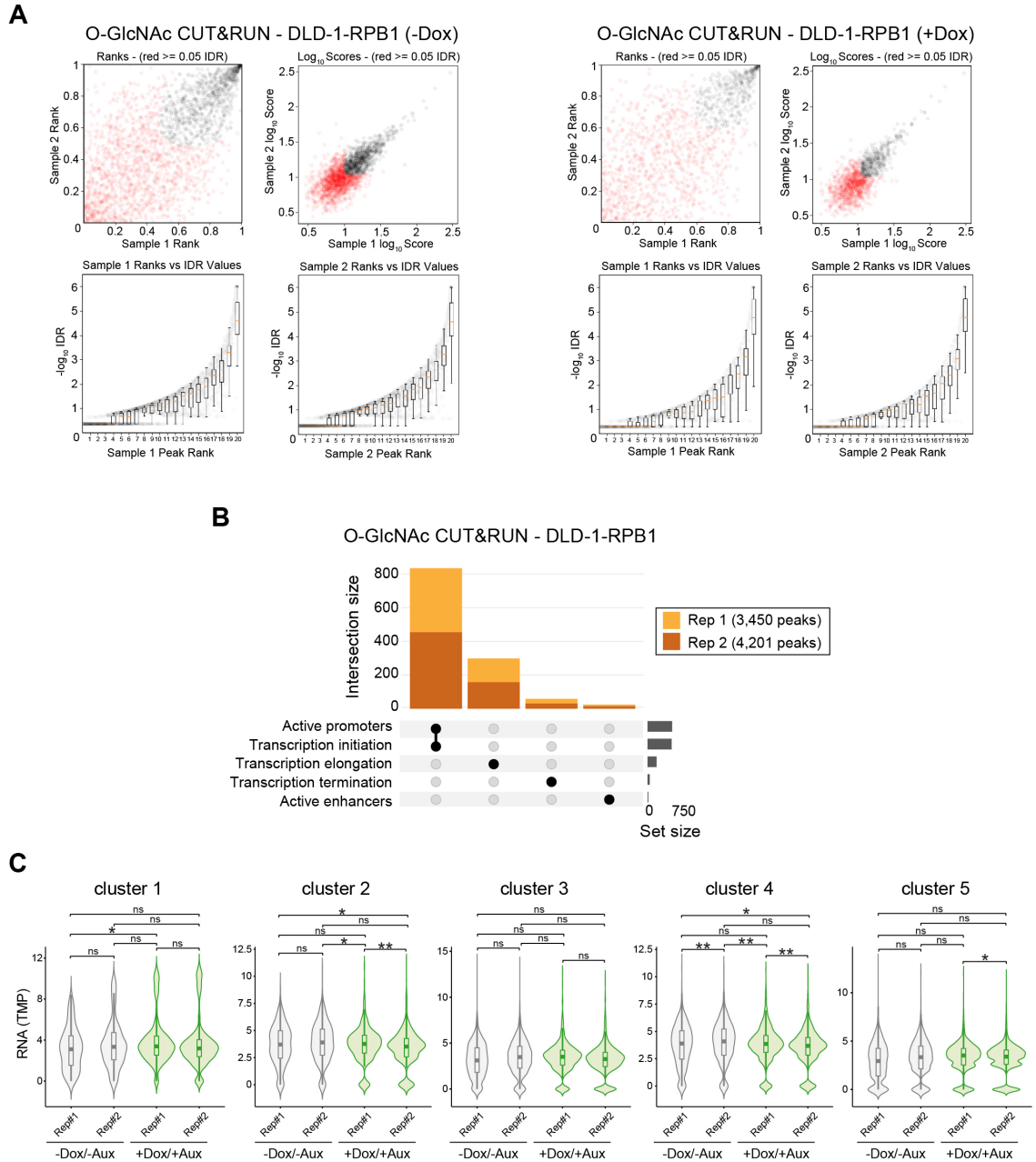


Fig. S3. O-GlcNAc profiling after RNA Pol II degradation in DLD-1 cells (*continued on page 7*)

A Irreproducible Discovery Rate (IDR) of the two CUT&RUN replicates in human DLD-1 cells before (3,450/4,201 peaks, left panel) and after (2,630/1,848 peaks, right panel) Dox treatment with significant IDR < 0.05 in black. **B** Upset plot of the location of O-GlcNAc CUT&RUN peaks in human DLD-1 cells without Doxycycline/Auxin (3,450 and 4,201 peaks for replicates 1 and 2) in functional genomic compartments: Active promoters (389/466 peaks), Transcription Initiation (381/456 peaks), Transcription Elongation (147/167 peaks), Transcription Termination (32/41 peaks) and active enhancers (10/14 peaks). O-GlcNAc preferentially occupies active promoters at the transcription initiation sites. **C** Violin plot showing gene expression levels after RNA Pol II degradation of the genes forming the 5 clusters shown in

Fig. 4D. The analysis is performed with generated RNA-seq expression data from DLD-1 cells (Mann-Whitney-Wilcoxon two-sided test. Non-significant (ns): $p > 0.05$; *: $p < 0.05$; **: $p < 0.01$).